Photoinduced Charge Separation of *N*,*N*,*N*′*N*′-Tetramethylbenzidine in Chromium Ion-Exchanged Zeolite X at Room Temperature

Koodali T. Ranjit* and Larry Kevan†

Department of Chemistry, University of Houston, Houston, Texas 77204-5003

Received: May 22, 2002; In Final Form: July 12, 2002

Chromium ion-exchanged zeolite X microporous materials were examined for the photoionization of *N*,*N*,*N*′*N*′-tetramethylbenzidine (TMB) with 320-nm irradiation at room temperature. Photoionization of chromium-containing zeolite X results in the formation of *N*,*N*,*N*′*N*′-tetramethylbenzidine radical cations ($TMB^{+\bullet}$), which are characterized by electron spin resonance (ESR) and diffuse reflectance spectroscopy (DRS). ESR studies indicate that Cr(V) acts as an electron acceptor. The photoyield and stability of the photoproduced $TMB^{+\bullet}$ cation radicals is higher in Cr(V)−X zeolite than in other hosts such as silica gels, zirconium phosphate, mordenite, and silicoaluminophosphates. The study delineates the importance of the size/shape features of the host system on the stability of the photoproduced $TMB^{+\bullet}$ cation radicals.

Introduction

The study of photoinduced charge separation in heterogeneous media is a subject that continues to attract attention.[1−3] Much research involves the development of systems that can sustain charge separation long enough so that the free energy of the photoproduced cation can be utilized to drive a chemical reaction. One of the main limitations in achieving long-lived charge separation is rapid back electron transfer. Back electron transfer results in the loss of the stored energy of the photoproduced cation into heat. Thus, an objective is to design systems in which long-lived charge separation can be achieved; furthermore, it is desirable to achieve this at room temperature.

With this objective, many systems have been examined as hosts to improve the efficiency of energy storage by minimizing back electron transfer. Heterogeneous systems can provide appropriate spatial organization of both donor and acceptor molecules to retard back electron transfer.[4−9] Appropriate tuning of the electronic and spatial properties of the host system can minimize back electron transfer. A gamut of systems ranging from micelles to mesoporous materials have been examined as hosts to improve the efficiency of photoinduced charge separation. Heterogeneous host systems such as micelles, vesicles, molecular sieves, silica gel, microporous silicoaluminophosphate (SAPO), and mesoporous MCM-41 silica have been found to be promising hosts compared to homogeneous solution systems.[10−15]

Microporous materials such as zeolites have evinced great interest as hosts for photoinduced charge separation. Zeolites have been a popular choice because their regular framework provides an appropriate spatial and electronic environment to retard back electron transfer.[16,17] The arrangement of cages and channels in these crystalline materials allows for the placement of molecules in well-defined and unique spatial arrangements. Several studies have focused on the steady-state photochemistry of trisbipyridine ruthenium(II) and bipyridinium ions in zeolites and have demonstrated a potential for long-lived charge separation.[4,7,8] Other examples where long-lived charge separation has been reported in zeolites include charge transfer between arenes as electron donors and viologens as electron acceptors.[18,19]

N,*N*,*N*′,*N*′-Tetramethylbenzidine (TMB) is characterized by a low gas-phase ionization potential (6.1−6.8 eV).[20] Photoionization of TMB in organic solvents and the formation of TMB cation radicals are well documented. Alkaitis and Grätzel first demonstrated the photoionization of TMB in organic solvents and micellar solutions.[21] $TMB^{+\bullet}$ can be produced in polar organic solvents by photolysis or by chemical oxidation. TMB can be easily oxidized by ultraviolet irradiation to form $TMB^{+\bullet}$.[22] The photoionization of TMB in micelles and vesicles has been the subject of numerous investigations in our laboratory.[23−27] However, the photoproduced TMB cation radical is not stable at room temperature, so previous studies to detect stable TMB cation radicals were carried out at 77 K.

Only a few reports exist on the photoionization of TMB in heterogeneous media.[12,28−30] Krishna et al. studied the photoionization of TMB incorporated into layered zirconium phosphate (ZrP).[28] However, TMB is incorporated only on the external surface of ZrP, which limits the use of this material as a host for efficient photoinduced charge separation. We have recently reported the photoinduced charge separation of TMB in Cr-incorporated SAPO materials.[29] The photoproduced $TMB^{+\bullet}$ cation radicals were characterized by electron spin resonance (ESR) and diffuse reflectance spectroscopy (DRS). ESR studies clearly seem to indicate the role of Cr(V) as an electron acceptor in SAPO materials. However, one drawback of SAPO materials is that the half-life of the photoproduced $TMB^{+\bullet}$ cation radicals is only about 3 h. Although the photoyield and stability of $TMB^{+\bullet}$ are much higher in Cr-containing SAPO materials than in other systems such as micelles and vesicles, it is desirable that the stability of the photoproduced cation radical be enhanced further. In the present investigation, we have explored photoinduced charge separation of TMB in zeolite X. TMB has molecular dimensions of about 5 Å × 13 Å. The zeolite X framework consists of sodalite cages that are connected tetrahedrally through double 6-rings to produce a 3D network. This arrangement gives rise to 13 Å-diameter supercages connected to each other through 12-

* Corresponding author. E-mail: kevan@uh.edu.
† Deceased June 4, 2002.

10.1021/jp021276r CCC: $22.00
Published on Web 08/16/2002

membered rings each having an opening of ~7 Å. Thus, such a host system can provide an appropriate spatial environment to accommodate and stabilize TMB.

Experimental Section

Preparation of Cr−X. Na−X (Grace Davison Chemicals, Baltimore, MD) was used as received. The zeolite samples were exchanged with 0.1 M sodium acetate to decrease any Fe(III) impurities. Chromium ions were incorporated into extraframework positions by liquid-state ion exchange. Liquid-state ion exchange was performed by adding 10 mL of 1×10^{-4} M $Cr(NO_3)_3$ to 2 g of Na−X zeolite, and the mixture was stirred overnight at room temperature. The samples were then filtered, washed with hot distilled water to remove any excess metal ions on the surface of the zeolite, and then dried in air to form Cr(III)−X materials. Three additional Cr−X materials containing different amounts of Cr(III) were prepared by varying the initial concentration of $Cr(NO_3)_3$. Cr(V)−X was formed by calcination of Cr(III)−X materials heated to 773 K and held at that temperature for ~14 h in static air. The materials were then cooled to room temperature slowly to form Cr(V)−X. H−X zeolite was prepared by exchanging Na^+ with NH_4^+ four times, followed by calcination.[31]

TMB Incorporation. TMB was incorporated by immersing 0.1 g of Cr−X in 1 mL of 1×10^{-2} M TMB in benzene for 12 h in the dark. Benzene was removed by flowing nitrogen gas for 1 h in the dark. For ESR measurements, 0.1 g of the sample was transferred into Suprasil quartz tubes (2-mm i.d. × 3-mm o.d.) that were sealed at one end. For preliminary studies, samples were evacuated below 1 Torr for ~1 h and flame sealed at the other end. The photoyield of samples evacuated to remove traces of oxygen, solvent (benzene), or water was similar to the photoyield of samples that were not evacuated. Hence, any such trace impurities do not seem to affect the results, and further photoionization experiments were carried out without evacuation. For DRS studies, the samples were loaded into a cylindrical quartz sample cell (22-mm diameter × 20-mm path length).

Characterization. X-ray diffraction powder patterns were recorded on a Siemens 5000 X-ray diffractometer using Cu Kα radiation of wavelength 1.541 Å in the range $10° < 2\theta < 50°$. Chemical analysis was performed by X-ray fluorescence analysis on a Kevex 770 XRF spectrometer. The composition of the Cr−X materials was determined by calibration with known standards to give the bulk composition. ESR spectra were recorded at room temperature at 9.5 GHz using a Bruker ESP 300 spectrometer with 100-kHz field modulation and low microwave power to avoid power saturation. Photoproduced $TMB^{+\bullet}$ yields were determined by double integration of the ESR spectra using the ESP 300 software. Each photoyield is an average of three ESR scans with a precision of less than 4%. The diffuse reflectance spectra were recorded at room temperature using a Perkin-Elmer model 330 spectrophotometer equipped with an integrating sphere. Thermal gravimetric analysis (TGA) of the samples was performed using a TGA 2050 analyzer (TA Instruments) in an oxygen atmosphere at a heating rate of 10 °C/min.

Photoirradiation. The TMB-containing Cr−X materials were irradiated using a 300-W Cermax xenon lamp (ILC-LX 300 UV) at room temperature. The incoming light was passed through a 10-cm water filter to block infrared radiation and through a Corning no. 7-54 filter to permit the passage of light of $\sim 1 \times 10^6$ erg cm^{-2} s^{-1} with a maximum wavelength at 320 ± 20 nm. The samples, sealed in a quartz tube, were placed in a quartz Dewar and rotated at 4 rpm to ensure even irradiation. The photoproduced $TMB^{+\bullet}$ cation radicals were identified by ESR and DRS.

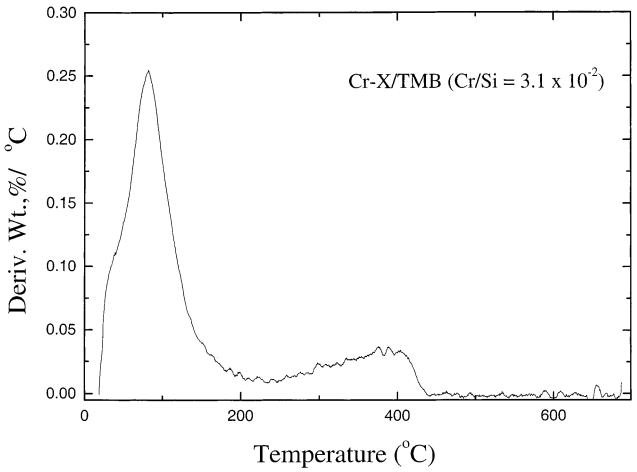

Figure 1. Thermal gravimetric analysis of Cr(V)−X (Cr/Si = 3.1×10^{-2}) with impregnated TMB.

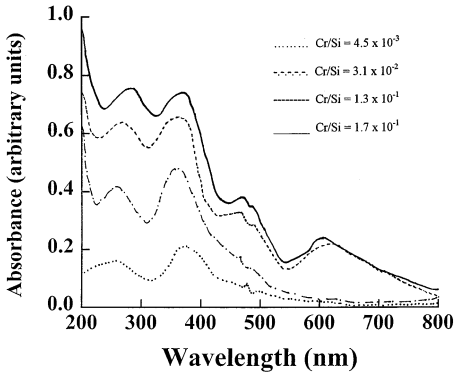

Figure 2. Diffuse reflectance spectra of calcined Cr−X materials.

TABLE 1: DRS Absorption Bands of Calcined Cr−X and Their Assignments

Cr/Si ratio	absorption bands (nm)	color	assignment
4.5×10^{-3}	252, 377, ~480 (weak shoulder)	pale yellow	Cr(V) and Cr(III)
3.1×10^{-2}	252, 362, ~480 (weak shoulder)	yellow	Cr(V) and Cr(III)
1.3×10^{-1}	270, 362, 468, 615	green	Cr(V) and Cr(III)
1.7×10^{-1}	288, 377, 468, 600	green	Cr(V) and Cr(III)

Results

Figure 1 shows TGA results obtained from the incorporation of TMB into Cr−X zeolite. The curves show two distinct weight losses. The first near 100 °C is attributed to water desorption from the external surface, and the second broad peak in the region from 300−430 °C is assigned to oxidative decomposition of TMB in flowing oxygen within the pores. The assignment of this peak to TMB decomposition is supported by its absence in flowing nitrogen. Thus, we can conclude from the TGA experiments that TMB penetrates into the pores of zeolite X.

The different oxidation states and coordination environments of Cr can be distinguished from each other by DRS and ESR. Table 1 gives the results of DRS absorption bands and the proposed assignments. Figure 2 shows the DRS spectra of the calcined Cr−X samples. As is evident from the Figure, the intensity of the band increases monotonically with the increase

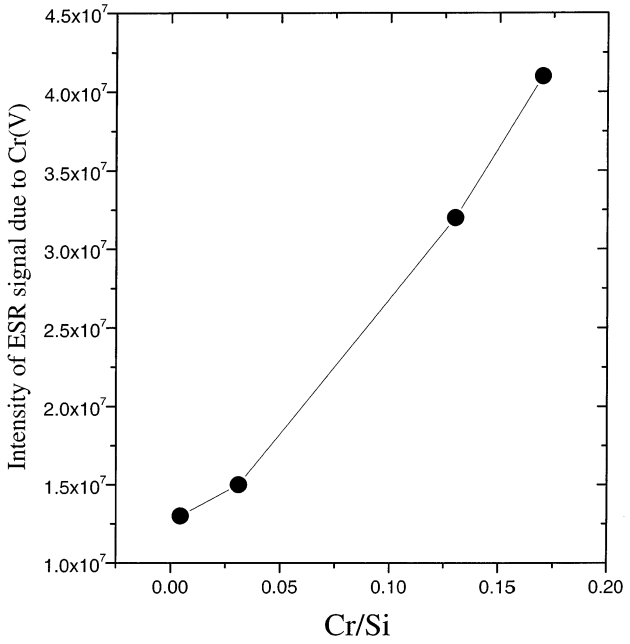

Figure 3. Intensity of ESR signal due to Cr(V) versus Cr content in calcined Cr−X materials.

in Cr content. From Figure 2, it is clear that the higher-energy bands (UV region) shift with the variation in Cr content; however, there is no uniform trend in the shift of the band position. For example, for Cr−X (Cr/Si = 4.5×10^{-3} and Cr/Si = 3.1×10^{-2}), the first band in the UV region appears at 252 nm; this band is shifted to 270 and 288 nm for Cr/Si ratios of 1.3×10^{-1} and 1.7×10^{-1}, respectively. Similarly, the second band in the UV region appears at ∼375 nm for Cr−X (Cr/Si = 4.5×10^{-3}), whereas it appears at ∼360 nm for Cr−X (Cr/Si = 3.1×10^{-2} and 1.3×10^{-1}); with further increases in Cr content, the band is shifted to ∼375 nm (Cr/Si = 1.7×10^{-1}).The higher-energy bands (252−288 and 362−377 nm) in the UV region are assigned to O → Cr(VI) charge-transfer bands that are typical of metallochromates.[32−38] It has been reported that in addition to chromates, chromyl cations $[Cr(V)]^{n+}$ and Cr_2O_3 clusters can also be formed on calcined surfaces, and the relative amounts of these species are support-, loading-, and treatment-dependent.[36] Thus, the oxidation state of Cr on an oxide support is strongly dependent on the pretreatment conditions (hydrated or dehydrated state, oxidizing environment in air or oxygen, reducing environment, et cetera) and on the type and composition of the support. It has been observed that Cr(V) is the main oxidized form in CrAPO-5 samples calcined in air at 500 °C.[39,40] Zhu et al.[41,42] have also observed that as-synthesized CrAPSO-11 and CrAPSO-5 showed an ESR spectrum assignable to Cr(III), but on calcination, the spectrum was assignable to Cr(V). Thus, we also attribute these bands to O → Cr(V) charge-transfer bands. We did not detect any Cr(VI) in our calcined samples. To test for Cr(VI) in extraframework positions, 0.2 g of calcined Cr−X was stirred in 10 mL of 1 M $Ca(NO_3)_3$ solution overnight. The solution was centrifuged, the centrifugate was collected, and 1 M of $AgNO_3$ was added dropwise to test for CrO_4^{2-}; however, we did *not* observe any precipitate due to Ag_2CrO_4. Bands in the UV region (250−310 and 310−400 nm) were earlier assigned to O → Cr(V) charge-transfer bands in CrO_4^{3-}-doped single crystals of Ca_2PO_4Cl and in Cr(V)-containing phosphates and vanadates.[43−45] Also consistent with the Cr(V) assignment is the fact that the intensity of the ESR signal at $g = 1.975$ due to Cr(V) increases with the Cr content, as shown in Figure 3. The

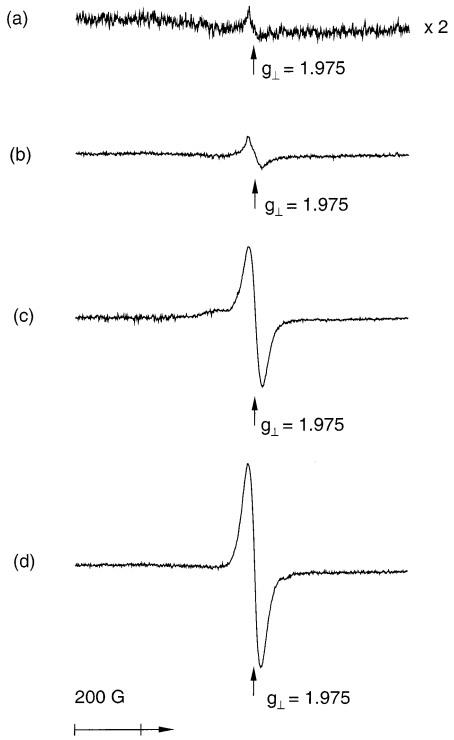

Figure 4. Room-temperature ESR spectra of Cr(V)−X samples: (a) Cr/Si = 4.5×10^{-3}, (b) Cr/Si = 3.1×10^{-2}, (c) Cr/Si = 1.3×10^{-1}, and (d) Cr/Si = 1.7×10^{-1}.

ESR studies described later also suggest that Cr(V) is present in the calcined samples. Also, no bands near 440 nm, which are usually due to dichromate species,[36] are observed in the present study. The bands observed in the visible region (∼470 nm and near 600 nm) for Cr−X zeolites having Cr/Si ratios of 1.3×10^{-1} and 1.7×10^{-1} are assigned to d−d transitions of Cr(III). These can be due to isolated Cr(III) ions or Cr_2O_3 clusters. The band near 600 nm is not observed for Cr−X samples having lower Cr contents (Cr/Si = 4.5×10^{-3} and 3.1×10^{-2}); however, a weak shoulder is observed in these samples near 480 nm. Because we did not detect Cr(VI) in any of the Cr−X samples, we believe that most Cr(III) ions on calcination in air at 550 °C are oxidized to Cr(V). The content of Cr(III) is lower than that of Cr(V), as can be concluded from the distinctly lower intensities of the corresponding band. However, at the moment, we are unable to quantify the amounts of Cr(V) and Cr(III) in the calcined Cr−X samples.

ESR Spectra. The ESR spectra of liquid-state ion-exchanged Cr−X (not shown) prior to calcination show a broad signal at $g = 1.98$ that is assigned to Cr(III), consistent with earlier reports. There is a significant broadening of the ESR lines of Cr(III) ($\Delta H_{pp} \approx 450$ G). Padlyak et al.[39] observed a considerable broadening in CrAPSO-5 samples ($\Delta H_{pp} \approx 450$ G), which has been related to dipolar interactions of the Cr(III) ions. After calcination, a very sharp signal at $g = 1.975$ is observed. This signal is assigned to a $g_\perp$ component of Cr(V) in either distorted octahedral or square-pyramidal coordination. Figure 4 shows the room-temperature ESR spectra of calcined Cr(V) samples. From Figure 4, we can see that the intensity of the signal at $g = 1.975$ increases with Cr content whereas the line width does not change with Cr content. According to the g equations for square-pyramidal geometry, $g_\perp = g_e - 2\lambda/\Delta_o$ and $g_\parallel = g_e - 8\lambda/\Delta_1$ where λ is the spin−orbit coupling constant of 160 cm^{-1} for Cr(V) in an oxide environment.[46] Δ_o and Δ_1 and are the two lowest-energy ultraviolet transitions of calcined, hydrated Cr−X. The calculated g values are $g_\perp = 1.980$ and $g_\parallel = 1.946$.

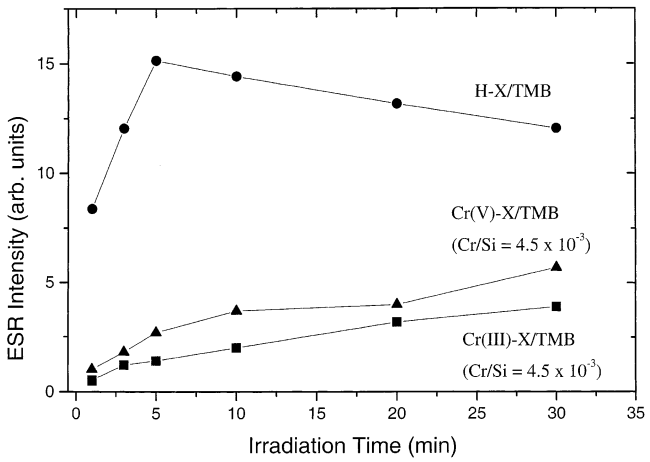

Figure 5. Room-temperature photoinduced $TMB^{+\bullet}$ cation radical yield measured by ESR versus irradiation time for Cr(III)−X (Cr/Si = 4.5×10^{-3}), Cr(V)−X (Cr/Si = 4.5×10^{-3}), and H−X samples.

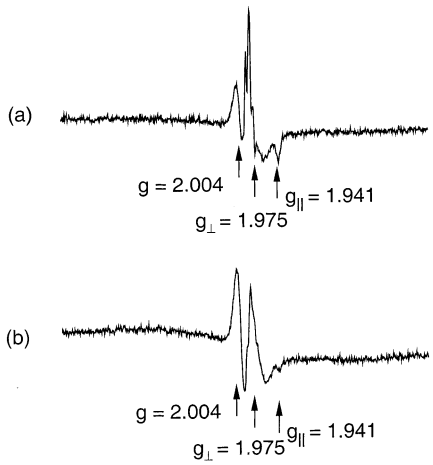

Figure 6. ESR spectra of Cr(V)−X (Cr/Si = 3.1×10^{-2}) at room temperature upon UV irradiation at 300 nm for (a) 0 min and (b) 30 min.

This $g_{\perp}$ value is in good agreement with the experimentally observed value of $g_{\perp} = 1.975$ at room temperature, which supports the assignment of the ESR spectrum to square-pyramidal Cr(V). The expected $g_{||}$ feature near $g = 1.95$ is apparently too weak to be observed at room temperature. The lack of resolution may be due to the spin-exchange effect or the *g*-strain broadening process, as discussed by Dalal et al.[47−49] At 77 K, the ESR spectrum of Cr−X (Cr/Si = 1.7×10^{-1}) shows a sharp signal at $g = 1.975$ that is assigned to the $g_{\perp}$ component and a weak signal at $g = 1.941$ that is assigned to a $g_{||}$ component. These experimental *g* values are in good agreement with the calculated *g* values and support the assignment of square-pyramidal Cr(V). For octahedral geometry, $g_{\perp} < g_{||}$, which does not agree with the experimental *g* parameters.

McGarvey[50] has shown that for a purely ionic model in which the unpaired electron occupies a d_{x2-y2} orbital and if the symmetry is axial, then $g_{\perp} = 1.96$ and $g_{||} = 1.91$. These values are lower than the observed values of $g_{\perp} = 1.975$ and $g_{||} = 1.941$, suggesting that some covalent bonding should be included. The fact that $g_{\perp} > g_{||}$ suggests that the ground state may be $d_{x^2-y^2}$ rather than d_{z^2}. This is interesting because in many cases (Li_3PO_4, Li_2AsO_4) the ground state is found to be d_{z^2}, as discussed by Greenblatt.[51] Dalal[52] has reported that in hydrated Cr(V) compounds such as Li_3CrO_8, Cs_3CrO_8, and Na_3CrO_8 $g_{\perp} > g_{||}$ and the ground state is $d_{x^2-y^2}$ rather than d_{z^2}. We have also observed a similar situation in the present study. Assignments of Cr(V) in various supports in square-pyramidal coordination with $g_{\perp} \approx 1.98$ and $g_{||} \approx 1.94$ have been reported by several groups.[29,34,37,41,42] Peroxy chromates containing Cr(V) have been extensively characterized by X-, Q-, and W-band ESR studies.[47−49,53−56] The *g* values were found to vary, depending on the sample characteristics. For example, for a K_3CrO_8 crystal, $g_{\perp} = 1.9854$ and $g_{||} = 1.9433$.[47] However, for 0.26% K_3CrO_8 in K_3NbO_8 powder, $g_{\perp} = 1.9848$ and $g_{||} = 1.9428$.

Photoionization Studies. The ESR spectra of TMB-impregnated Cr(III) liquid-state ion-exchanged zeolite X, Cr(III)−X/TMB, show signals at $g = 2.004$ due to $TMB^{+\bullet}$ after irradiation. The intensity of the signal at $g = 1.98$ due to Cr(III) is much weaker than the signal at $g = 2.004$ assigned to the $TMB^{+\bullet}$ cation radical. Figure 5 shows the changes in the intensity of the ESR signal due to $TMB^{+\bullet}$ in Cr(III)−X (Cr/Si = 4.5×10^{-3}). In previous studies, we have observed enhanced stability of PC_1^+ and $TMB^{+\bullet}$ cation radicals in Cr(V)-containing SAPO-5 compared to Cr(III) -containing SAPO-5.[29] Hence, it is of interest to study the photoionization of TMB in Cr(V)−X samples. The ESR spectra of calcined Cr(V)−X (Cr/Si = 4.5×10^{-3}) show a signal at $g = 1.975$ assigned to Cr(V). On impregnation of TMB (prior to irradiation), a new, strong signal at $g = 2.004$ assigned to the $TMB^{+\bullet}$ cation radical is seen. This indicates that some $TMB^{+\bullet}$ cation radicals are produced during sample preparation. After being irradiated at room temperature for 5 min, the samples show very strong ESR signals at $g = 2.004$. The intensity of the signal at $g = 1.975$ due to Cr(V) is weaker than the signal at $g = 2.004$ due to $TMB^{+\bullet}$ for Cr(V)−X (Cr/Si = 4.5×10^{-3}). With further increases in the irradiation time, the intensity of the signal at $g = 2.004$ increases and remains constant after 30 min of irradiation. An irradiation time of 30 min was hence selected for comparative photoyield and stability studies. A change in the color of Cr(V)−X/TMB is seen; the sample prior to irradiation is pale yellow but turns pale green after irradiation. Green is a characteristic color of $TMB^{+\bullet}$ cation radicals in solid heterogeneous systems. The *g* value of 2.004 and the peak-to-peak line width of ∼20 G are similar to those of $TMB^{+\bullet}$ in other heterogeneous systems, so the ESR line at $g = 2.004$ is reasonably assigned to the $TMB^{+\bullet}$ cation radical. This confirms the photoionization of TMB to $TMB^{+\bullet}$.

Figure 5 shows the changes in the intensity of the ESR signal due to $TMB^{+\bullet}$ cation radicals in Cr(V)−X (Cr/Si = 4.5×10^{-3}) and H−X samples. From Figure 5, we see that the photoyield of $TMB^{+\bullet}$ is higher in Cr(V)−X than in Cr(III)−X. For H−X/TMB, the dark reaction is significantly higher than that of Cr−X. The ESR intensity increases rapidly during the first 5 min of irradiation, but on further irradiation, the intensity of the ESR signal continues to decrease. This suggests that the photoproduced $TMB^{+\bullet}$ cation radical is not stabilized in the H−X zeolite framework and that Cr−X is a better host than H−X for forming and stabilizing $TMB^{+\bullet}$ cation radicals. Also, the color of H−X/TMB fades completely in about 1 h, indicating poor stability of the photoinduced $TMB^{+\bullet}$ radical in H−X.

To understand the influence of Cr content on the photoyield and stability of the photoproduced $TMB^{+\bullet}$ cation radicals, the photoionization of TMB was carried out in Cr(V)−X samples with different amounts of Cr. Figure 6 shows the ESR spectra of Cr−X/TMB (Cr/Si = 3.1×10^{-2}) before and after ultraviolet irradiation at room temperature. The ESR spectra show three signals: one at $g = 2.004$ due to the $TMB^{+\bullet}$ cation radical, another at $g = 1.975$ assigned to a $g_{\perp}$ component of Cr(V), and the third at $g = 1.941$ assigned to the $g_{||}$ component of Cr(V).

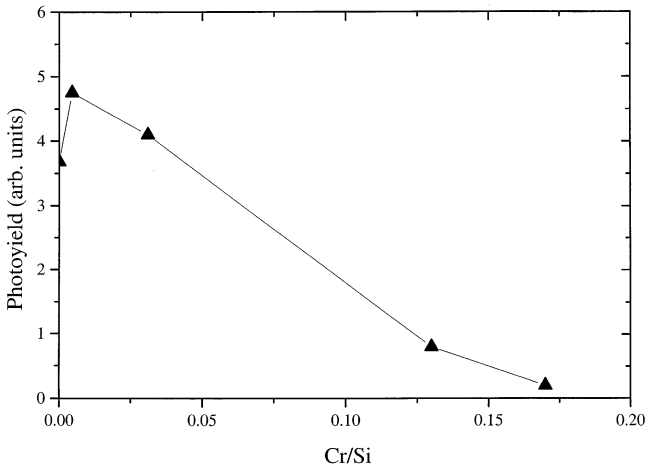

Figure 7. Room-temperature photoinduced $TMB^{+\bullet}$ cation radical yield measured by ESR versus Cr/Si ratio for Cr(V)−X/TMB.

For Cr−X/TMB samples with Cr/Si ratios of 3.1×10^{-2}, 1.3×10^{-1}, and 1.7×10^{-1}, the ESR signals due to the $TMB^{+\bullet}$ cation radical and Cr(V) partially overlap. A direct measurement of the signal intensity for the $TMB^{+\bullet}$ cation radical by double integration is hence not accurate. The relative intensity for the $TMB^{+\bullet}$ cation radical was estimated in the following manner for these three samples. The signals before irradiation were subtracted from the signals after irradiation, and the relative intensity of the $TMB^{+\bullet}$ cation was estimated from the height of the resulting line at $g = 2.004$. This method of calculating the relative intensity of the photoproduced $TMB^{+\bullet}$ cation radicals seems fairly reliable because the height of the signal at $g = 2.004$ gives an approximate measure of the amount of $TMB^{+\bullet}$ radical cations.

After 30 min of irradiation, there seems to be an increase in the relative intensity of the peak at $g = 2.004$ and a decrease in the relative intensity of the peaks at $g = 1.975$ and 1.941. The ESR studies thus seem to suggest that Cr(V) acts as an electron acceptor. Figure 7 shows the photoyield of $TMB^{+\bullet}$ versus the Cr content. It is evident that the maximum photoyield is obtained for Cr(V)−X having the lowest Cr content, namely, Cr/Si = 4.5×10^{-3}. On increasing the Cr concentration, the photoyield decreases. This is attributed to the formation of greater amounts of $(TMB)_2^{2+}$ in the Cr(V)−X samples having Cr/Si > 4.5×10^{-3}. Evidence for this comes from DRS results, which are discussed below. In addition, the photoproduced $TMB^{+\bullet}$ cation radicals are stable for days if not weeks in Cr(V)−X zeolites. This is a marked improvement over the stability of $TMB^{+\bullet}$ cation radicals in silica gels, ZrP, SAPO-5, SAPO-8, SAPO-11, and mordenite reported earlier where the half-lives of the photoproduced $TMB^{+\bullet}$ cation radicals range from about 3 h to 2 days.[12,28,29]

Diffuse reflectance spectroscopy studies of the Cr(V)−X/TMB samples are shown in Figures 8 and 9. Figure 8 shows the DRS spectra of Cr(V)−X/TMB (Cr/Si = 4.5×10^{-3}). The solid line shown is the diffuse reflectance spectrum of Cr(V)−X/TMB before irradiation. The absorption peak at 300 nm is assigned to neutral TMB molecules. In addition, there is a very weak absorption with characteristic vibronic fine structure in the 400−500-nm region. This is due to the formation of $TMB^{+\bullet}$ cation radicals during sample preparation and is consistent with the ESR results that indicate that some $TMB^{+\bullet}$ cation radicals are produced prior to irradiation. Also, a small shoulder is seen near 270 nm, which is assigned to a O → Cr(V) charge-transfer band. After 5 min of irradiation, there is a significant increase in the absorption from 380 to 500 nm, and a new broad band

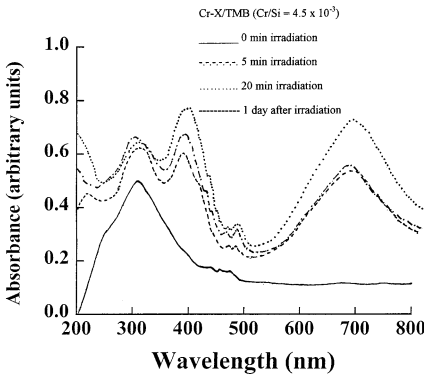

Figure 8. Diffuse reflectance spectra of Cr(V)−X/TMB (Cr/Si = 4.5×10^{-3}) at room temperature upon UV irradiation.

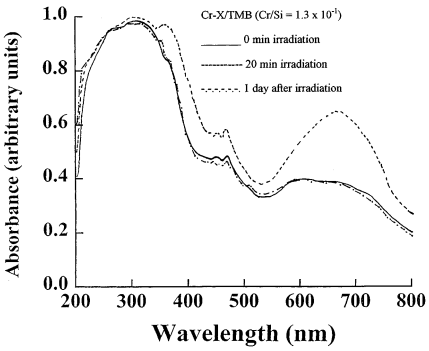

Figure 9. Diffuse reflectance spectra of Cr(V)−X/TMB (Cr/Si = 1.3×10^{-1}) at room temperature upon UV irradiation.

in the 600 to 800-nm region centered at ∼700 nm appears. This is assigned to trapped electrons in Cr(V)−X. Also, the color of the sample changes from pale yellow to pale green. The increase in the absorption from 400 to 500 nm indicates an increase in the concentration of $TMB^{+\bullet}$. Also, there is a new absorption near 400 nm between the absorption peaks due to TMB and $TMB^{+\bullet}$. This may indicate the existence of $(TMB)_2^{2+}$, which is a charge-transfer complex that has an absorption peak near 385 nm.[57] On further irradiation, there is only a small increase in the absorptions due to $TMB^{+\bullet}$, $(TMB)_2^{2+}$, and trapped electrons. After storing the sample at room temperature in the dark for 1 day, there is a decrease in the absorption due to $TMB^{+\bullet}$, $(TMB)_2^{2+}$, and trapped electrons. The DRS of Cr(V)−X (Cr/Si = 3.1×10^{-2}) shows similar features to those described for Cr(V)−X (Cr/Si = 4.5×10^{-3}).

Figure 9 shows the DRS of Cr(V)−X/TMB (Cr/Si = 1.3×10^{-1}). Before irradiation, DRS shows peaks in the 420 to 500 nm region due to $TMB^{+\bullet}$ produced in the dark. The broad absorption in the 550 to 800 nm region is due to d−d transitions of Cr(III). The weak shoulders at 270 and 370 nm are due to O → Cr(V) charge-transfer bands, as discussed earlier. The band seen near 300 nm is due to TMB. After irradiating the sample for 20 min, there is an increase in the absorption from 420 to 500 nm due to an increase in $TMB^{+\bullet}$ concentration and the appearance of a new broad band centered near 650-nm due to trapped electrons. In addition, there is an increase in the absorption near 370 nm assigned to $(TMB)_2^{2+}$. After the sample has been stored in the dark at room temperature for 1 day, the spectrum shows features similar to those observed prior to irradiation. A comparison of Figures 8 and 9 shows that the stability of photoproduced $TMB^{+\bullet}$ in Cr(V)−X (Cr/Si = 1.3×10^{-1}) is lower than in Cr(V)−X (Cr/Si = 4.5×10^{-3}). The DRS of Cr(V)−X (Cr/Si = 1.7×10^{-1}) shows features similar to those of Cr(V)−X (Cr/Si = 1.3×10^{-1}) before and after irradiation.

Discussion

The ESR results suggest that Cr is predominantly present as Cr(V) in calcined Cr−X, probably in square-pyramidal coordination, in addition to some amount of Cr(III). On the basis of DRS studies and other reports of Cr(V) in phosphate and vanadate hosts[43−45] and the failure to detect Cr(VI) in calcined Cr−X, the bands in the UV region are attributed to O → Cr(V) charge-transfer bands rather than to O → Cr(VI) charge-transfer bands.

The ESR and DRS results clearly confirm the photooxidation of TMB molecules to $TMB^{+\bullet}$ cation radicals in Cr ion-exchanged zeolite X at room temperature. The increase in the intensity of the ESR signal due to $TMB^{+\bullet}$ cation radicals with time for calcined ion-exchanged Cr(V)−X materials suggests that Cr(V) assists the photoionization of TMB. Other evidence for the role of the Cr(V) ion as the electron acceptor comes from the fact that the total ESR intensity of the sample prior to and after incorporation of TMB remains the same, although a decrease in the spin concentration of Cr(V) is observed. After 30 min of irradiation, there is an increase in the relative intensity of the signal at $g = 2.004$ due to $TMB^{+\bullet}$ and decreases in the relative intensities of the signals at $g_\perp = 1.975$ and $g_{||} = 1.941$ due to Cr(V), as indicated by reaction 1.

$$\mathrm{Cr(V)} + \mathrm{TMB} \rightarrow \mathrm{Cr(IV)} + \mathrm{TMB}^{+\bullet} \qquad (1)$$

In addition, when Cr−X/TMB is stored in the dark after irradiation, the relative intensity of the signal at $g = 2.00$ due to $TMB^{+\bullet}$ decreases, and simultaneously, the relative intensities of the ESR signals at $g_\perp = 1.975$ and $g_{||} = 1.941$ due to Cr(V) increase according to back electron transfer reaction 2.

$$\mathrm{Cr(IV)} + \mathrm{TMB}^{+\bullet} \rightarrow \mathrm{Cr(V)} + \mathrm{TMB} \qquad (2)$$

These points clearly suggest that Cr(V) acts as an electron acceptor and assists in stabilizing the $TMB^{+\bullet}$ cation radical. Another feature of the Cr(V)−X/TMB materials is that the ESR signal from the less-abundant chromium isotope (^{53}Cr) with $I = {}^3/_2$ (9.5%) is observed as a quartet pattern. Such lines are also observed in oxochromium(V) porphyrin complexes.[58] The photoyield and stability of the $TMB^{+\bullet}$ cation radical is higher in calcined ion-exchanged samples than in only ion-exchanged samples. ESR studies show that Cr mainly exists as Cr(III) in liquid-state ion-exchanged Cr−X whereas Cr exists as Cr(V) in calcined Cr−X. The higher photoyield and the greater stability of the photoproduced $TMB^{+\bullet}$ cation radicals in Cr(V)−X can be rationalized on the basis of the higher electron affinity of Cr(V) ($E°$[Cr(V/IV)] = 1.340 V) as compared to that of Cr(III) ($E°$[Cr(III/II)] = −0.407 V). The reduction potential of Cr(III) is negative, making the reaction less favorable than that of Cr-(V). Alkaitis et al.[59] also observed a dependence of the electron-transfer rates from phenothiazine to metal ion acceptors in micellar solutions and correlated the results obtained with the reduction potentials of the metal ions.

The stability of the photoproduced $TMB^{+\bullet}$ cation radicals is much higher in Cr(V)−X ($t_{1/2} \approx 10-30$ days) than in other oxide hosts investigated earlier in our laboratory such as silica gel, ZrP, SAPO-5, SAPO-8, SAPO-11, and mordenite. Thus, the photooxidation mechanism of $TMB^{+\bullet}$ cation radicals in Cr-(V)-containing zeolite X is more efficient than in other oxide hosts.

H−X/TMB shows weak ESR signals after 30 min of irradiation, suggesting that the protons in H−X may act as electron acceptors. Low-temperature measurements at 77 K were made to detect trapped hydrogen atoms, but none were seen. This is consistent with an earlier report wherein signals due to hydrogen atoms are observed only in large-pore materials.[60]

Although Cr(V)-containing zeolite X is an efficient host for the formation and stabilization of $TMB^{+\bullet}$ cation radicals, the photoyield decreases as the Cr content increases. This is in contrast to our earlier studies wherein we observed an initial increase in the photoyield with an increase in Cr content followed by a decrease in the photoyield with further increases in Cr content.[29] To understand this trend, DRS studies were carried out. XRD and DRS studies do not reveal the presence of a chromium oxide phase in any of the Cr(V)−X samples. The ESR studies show that the decay curves for the $TMB^{+\bullet}$ cation radical in all Cr(V)−X samples could be fit by a first-order exponential decay. Also, the ESR spectra of the Cr(V)−X/TMB samples are symmetric, suggesting the presence of only one paramagnetic species, namely, the $TMB^{+\bullet}$ cation radical. This indicates that the decrease in the photoyield on increasing the Cr content may be due to the formation of nonparamagnetic species.

The DRS studies of Cr(V)−X/TMB samples show an additional peak at ∼380 nm between the peaks due to neutral TMB molecules (300 nm) and $TMB^{+\bullet}$ cation radicals (420−500 nm). This peak is assigned to the nonparamagnetic diamine−diimine charge-transfer complex $(TMB)_2^{2+}$. Awano et al.[57,61] have suggested that the oxidation of TMB leads to the formation of a band at ∼375 nm assigned to a charge-transfer complex consisting of a neutral TMB molecule as a donor and a TMB^{2+} cation as an acceptor. TMB^{2+} acts as a strong electron acceptor and has either a diiminium or quinoid structure. Our results are similar to the results obtained by Awano et al., and hence the assignment of the band at ∼380 nm to $(TMB)_2^{2+}$ seems credible. The intensity of the band at ∼380 nm increases as the Cr content increases. Hence, the photoyield and stability of the $TMB^{+\bullet}$ cation radical decrease as the Cr content increases. The half-life of the photoproduced $TMB^{+\bullet}$ cation radicals ranges from 10 days ($Cr/Si = 1.7 \times 10^{-1}$) to 30 days ($Cr/Si = 4.5 \times 10^{-3}$). Both of these values are much longer than the half-lives of $TMB^{+\bullet}$ in amorphous silica gel of about 2 h and in ZrP of about 10 h.

TMB molecules and $TMB^{+\bullet}$ radical cations do not absorb in the 500−800-nm region. Hydrated electrons typically absorb between 600 and 700 nm. There is a significant absorption near 650 nm after irradiation of Cr(V)−X materials. This is assigned to trapped electrons in Cr(V)−X zeolite. This band is removed by typical electron scavengers such as acetone, supporting the assignment of this band. The trapped electron should be visible in the ESR spectrum. However, the signal at $g = 2.00$ due to $TMB^{+\bullet}$ clearly precludes the observation of these presumedly trapped electrons by ESR.

Conclusions

Cr(V)-containing zeolite X microporous materials were evaluated for the photoionization of TMB. The $TMB^{+\bullet}$ cation radical yield was found to depend on the electron affinity and the Cr content. ESR studies indicate that Cr(V) is an electron acceptor. The stability of $TMB^{+\bullet}$ cation radicals in Cr(V)−X zeolite is found to be longer than in other oxide hosts. The results clearly indicate that Cr(V)-containing zeolite X provides an appropriate steric and electrostatic environment to minimize back electron transfer and increase the lifetime of photogenerated $TMB^{+\bullet}$ cation radicals to many days or even weeks at room temperature.

Acknowledgment. This research was supported by the Chemical Sciences, Geosciences and Biosciences Division,

Office of the Basic Energy Sciences, Office of Science, U.S. Department of Energy, the Texas Advanced Research Program, and the Environmental Institute of Houston.

References and Notes

(1) Gust, D.; Moore, T. A.; Moore, A. L. *Acc. Chem. Res*. **2001**, *34*, 40.
(2) Ipe, B. I.; Thomas, K. G.; Barazzouk, S.; Hotchandani, S.; Kamat, P. V. *J. Phys. Chem. B* **2002**, *106*, 18.
(3) Scaiano, J. C.; Garcia, H. *Acc. Chem. Res.* **1999**, *32*, 783.
(4) Borja, M.; Dutta, P. K. *Nature (London)* **1993**, *362*, 43.
(5) *Kinetics and Catalysis in Microheterogeneous Systems*; Grätzel, M., Kalyanasundaram, K., Eds.; Marcel Dekker: New York, 1991.
(6) *Photochemistry in Organized and Constrained Media*; Ramamurthy, V., Ed.; VCH: New York, 1991.
(7) Sykora, M.; Kincaid, J. R. *Nature (London)* **1997**, *387*, 162.
(8) Krueger, J. S.; Mayer, J. E.; Mallouk, T. E. *J. Am. Chem. Soc.* **1988**, *110*, 8232.
(9) Gessner, F.; Scaiano, J. C. *J. Photochem. Photobiol., A* **1992**, *67*, 91.
(10) Infelta, P. P.; Grätzel, M.; Fendler, J. H. *J. Am. Chem. Soc*. **1980**, *102*, 1479.
(11) Kang, Y. S.; Kevan, L. *J. Phys. Chem.* **1994**, *98*, 4389.
(12) Xiang, B.; Kevan, L. *Colloids Surf., A* **1993**, *72*, 11.
(13) Matsuura, K.; Kevan, L. *J. Phys. Chem.* **1996**, *100*, 10652.
(14) Ranjit, K. T.; Kevan, L. *J. Phys. Chem. B* **2001**, *105*, 118.
(15) Sinlapadech, S.; Krishna, R. M.; Kevan, L. *J. Phys. Chem. B* **2001**, *105*, 4350.
(16) Ramamurthy, V.; Eaton, D. F.; Caspar, J. V. *Acc. Chem. Res.* **1992**, *25*, 299.
(17) *Introduction to Zeolite Science and Practice*; van Bekkum, H., Flanigen, E. M., Jansen, J. C., Eds.; Elsevier: Amsterdam, 1991.
(18) Yoon, K. B.; Hubig, S. M.; Kochi, J. K. *J. Phys. Chem.* **1994**, *98*, 3865.
(19) Park, Y. S.; Um, S. Y.; Yoon, K. B. *J. Am. Chem. Soc*. **1999**, *121*, 3193.
(20) Fulton, A.; Lyons, L. E. *Aust. J. Chem.* **1968**, *21*, 873.
(21) Alkaitis, S. A.; Grätzel, M. *J. Am. Chem. Soc*. **1976**, *98*, 3549.
(22) Lewis, A. N.; Lipkin, D. *J. Am. Chem. Soc*. **1942**, *64*, 2801.
(23) Narayana, P. A.; Li, A. S. W.; Kevan, L. *J. Am. Chem. Soc*. **1982**, *104*, 6502.
(24) Arce, R.; Kevan, L. *J. Chem. Soc., Faraday Trans. 1* **1985**, *81*, 1025.
(25) Li, A. S. W.; Kevan, L. *J. Am. Chem. Soc*. **1983**, *105*, 5752.
(26) Narayana, P. A.; Li, A. S. W.; Kevan, L. *J. Am. Chem. Soc*. **1981**, *1034*, 3603.
(27) Stenland, C.; Kevan, L. *J. Phys. Chem.* **1993**, *97*, 10498.
(28) Krishna, R. M.; Kevan, L. *Microporous Mesoporous Mater*. **1999**, *32*, 169.
(29) Ranjit, K. T.; Kevan, L. *Phys. Chem. Chem. Phys.* **2001**, *3*, 2921.
(30) Bae, J. Y.; Ranjit, K. T.; Choo, H.; Kevan, L. *Phys. Chem. Chem. Phys.* **2001**, *3*, 5602.
(31) Baldovi, M. F.; Cozens, F. L.; Fornes, V.; Garcia, H.; Scaiano, J. C. *Chem. Mater*. **1996**, *8*, 152.
(32) Weckhuysen, B. M.; De Ridder, L. M.; Schoonheydt, R. A. *J. Phys. Chem.* **1993**, *97*, 4756.
(33) Weckhuysen, B. M.; Verberckmoes, An. A.; Buttiens, An. L.; Schoonheydt, R. A. *J. Phys. Chem.* **1994**, *98*, 579.
(34) Weckhuysen, B. M.; De Ridder, L. M.; Grobet, P. J.; Schoonheydt, R. A. *J. Phys. Chem.* **1995**, *99*, 320.
(35) Weckhuysen, B. M.; Schoofs, B.; Schoonheydt, R. A. *J. Chem. Soc., Faraday Trans.* **1997**, *93*, 2117.
(36) Weckhuysen, B. M.; Wachs, I. E.; Schoonheydt, R. A. *Chem. Rev.* **1996**, *96*, 3327.
(37) Weckhuysen, B. M.; Schoonheydt, R. A.; Mabbs, F. E.; Collison, D. *J. Chem. Soc., Faraday Trans.* **1996**, *92*, 2431.
(38) Weckhuysen, B. M.; Schoonheydt, R. A. *Zeolites* **1994**, *14*, 360.
(39) Padlyak, B. V.; Kornatowski, J.; Zadrozna, G.; Rozwadowski, M.; Gutsze, A. *J. Phys. Chem. A* **2000**, *104*, 11837.
(40) Kornatowski, J.; Zadrozna, G.; Rozwadowski, M.; Zibrowius, B.; Marlow, F.; Lercher, J. A. *Chem. Mater*. **2001**, *13*, 4447.
(41) Zhu, Z.; Kevan, L. *J. Phys. Chem. B* **1997**, *101*, 10763.
(42) Zhu, Z.; Kevan, L. *Phys. Chem. Chem. Phys.* **1999**, *1*, 199.
(43) Banks, E.; Greenblatt, M.; Holt, S. *J. Chem. Phys.* **1968**, *49*, 1431.
(44) Simo, C.; Banks, E.; Holt, S. L. *Inorg. Chem.* **1970**, *9*, 183.
(45) Milstein, J. B.; Ackerman, J.; Holt, S. L.; McGarvey, B. R. *Inorg. Chem.* **1972**, *11*, 1178.
(46) Kivelson, D.; Lee, S. K. *J. Chem. Phys.* **1964**, *41*, 1896.
(47) Dalal, N. S.; Millar, J. M.; Jagadeesh, M. S.; Seehra, M. S. *J. Chem. Phys.* **1981**, *74*, 1916.
(48) Dalal, N. S.; Suryan, M. M.; Seehra, M. S. *Anal. Chem.* **1981**, *53*, 953.
(49) Cage, B.; Hassan, A. K.; Pardi, L.; Krzystek, J.; Brunel, L.-C.; Dalal, N. S. *J. Magn. Reson.* **1997**, *124*, 495.
(50) McGarvey, B. R. *J. Chem. Phys.* **1962**, *37*, 2001.
(51) Greenblatt, M. *J. Chem. Educ.* **1980**, *54*, 546.
(52) Cage, B.; Geyer, W.; Abboud, K. A.; Dalal, N. S. *Chem. Mater*. **2001**, *13*, 871.
(53) Cordischi, D.; Campa, M. C.; Indovina, V.; Occhiuzzi, M. *J. Chem. Soc., Faraday Trans.* **1994**, *90*, 207.
(54) Cordischi, D.; Indovina, V.; Occhiuzzi, M. *J. Chem. Soc., Faraday Trans.* **1991**, *87*, 3443.
(55) Cage, B.; Weekley, A.; Brunel, L.-C.; Dalal, N. S. *Anal. Chem.* **1999**, *71*, 1951.
(56) Cage, B.; Dalal, N. S. *Chem. Mater*. **2001**, *13*, 880.
(57) Awano, H.; Ogata, T.; Murakami, H.; Yamashita, T.; Ohigashi, H. *Synth. Met.* **1990**, *36*, 263.
(58) Fujii, H.; Yoshimura, T.; Kamada, H. *Inorg. Chem*. **1997**, *36*, 1122.
(59) Alkaitis, S. A.; Beck, G.; Grätzel, M. *J. Am. Chem. Soc.* **1975**, *97*, 5723.
(60) Xiang, B.; Kevan, L. *Langmuir* **1994**, *10*, 2688.
(61) Awano, H.; Ohigashi, H. *Synth. Met.* **1989**, *32*, 389.